



N-doped ZnO as an efficient photocatalyst for thiocyanation of indoles and phenols under visible-light

Mona Hosseini-Sarvari¹ · Abdollah Masoudi Sarvestani¹

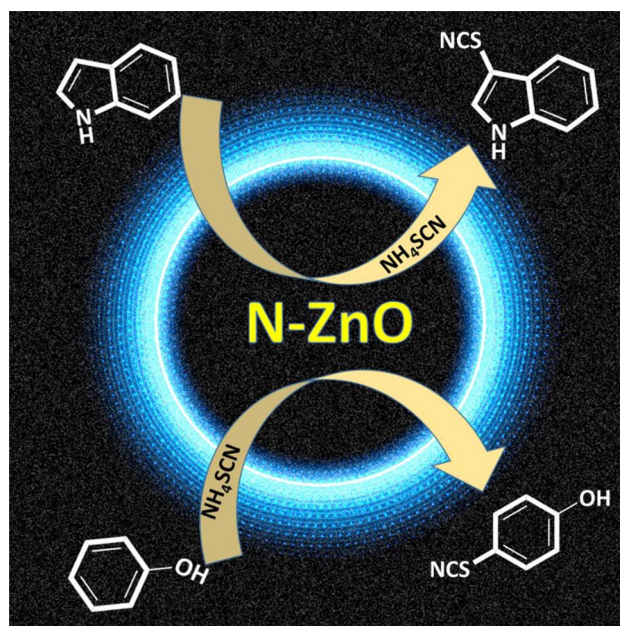
Received: 6 March 2021 / Accepted: 21 June 2021 / Published online: 9 July 2021

© The Author(s), under exclusive licence to European Photochemistry Association, European Society for Photobiology 2021

Abstract

In this study, nitrogen-doped ZnO nanorods (N–ZnO NRs) were synthesized via a very simple hydrothermal process, fully characterized, and this photocatalyst was successfully exploited in thiocyanation reactions of indoles and phenols at room temperature under visible light irradiation. Two important classes of aromatic compounds indoles, and phenols using N–ZnO NRs as photocatalyst treated with ammonium thiocyanate as thiocyanation agent formed the corresponding thiocyanate compounds in good yields. Nitrogen is one of the most appropriate p-type dopants that is nontoxic, similar to the atomic radius to oxygen, and lower electronegativity and ionization energy than the O atom. Therefore, the N doping converts ZnO into the p-type ZnO semiconductor structure. This potent, simple, and versatile protocol afforded thiocyanation reactions of indole and phenols under visible light. The reactions proceeded through a radical pathway by applying air molecular oxygen as a low cost and environmentally friendly terminal oxidant. The proposed mechanism based on control experiments was thoroughly described.

Graphic abstract



Keywords N-doped ZnO · Photochemistry · Green chemistry · Indole · Phenol

✉ Mona Hosseini-Sarvari
hossaini@shirazu.ac.ir

Extended author information available on the last page of the article

1 Introduction

The semiconductor photocatalysis field as a branch of photochemistry has attracted a lot of attention in recent years due to its high potential to deliver valuable products. Indeed, this privileged approach could successfully change the harsh reaction conditions in milder using light as a cost-effective source. Particularly, researchers focused on performing photochemical reactions under visible light to meet green chemistry principles.

ZnO is one of the most promising semiconductors due to its unique properties such as broad bandgap, cost-effectiveness, high electron mobility, and non-toxicity [1–3]. Studies of ZnO hexagonal nanorod structure represent a significant research area, and it is reported that one-dimensional (1D) ZnO nanorod arrays could enhance photocatalytic efficiency [4]. One dimensional nanostructure, such as nanowires and nanorods, offers a higher surface-to-volume ratio compared to nanoparticulate coatings on a flat plate [5] which increases the photocatalytic efficiency. However, unfortunately, only UV light could activate ZnO to participate in photochemical reactions. The efficiency of photocatalysis depends upon the harvested region of the solar spectrum by ZnO nanostructures and the lifetime of the generated electron–hole pair. As ZnO is a wide bandgap semiconductor and its bandgap is in the UV region, thus it can only harvest the UV region. UV light is just 5% of the solar spectrum [6]. To improve efficiency, the first step is to harvest a larger spectrum of sunlight so that more electron–hole pairs can be generated. The second step is to improve the efficiency of a photon to electron conversion. The third step is to increase the lifetime of photogenerated electron–hole pairs. These issues could be successfully met by doping with other additives such as metal or non-metal ions, metal complexes, and organic dyes. In particular, N-doping is considered to be the most suitable p-type doping agent that has been successfully applied to modify ZnO for use in the visible-light region [7–9].

Traditionally, among non-metal elements, N has been considered as one of the most appropriate p-type dopants highly thanks to its nontoxicity, abundance similar to the atomic radius to that of O, and lower electronegativity and ionization energy than those of the O atom. The N doping helps to convert the n-type into the p-type ZnO semiconductor structure. As the nearly similar ionic radius of N to O, a strong contribution of mixing of its 2p orbital with 2p orbital of O helps in the bandgap narrowing which improves the photocatalytic activity [10, 11]. As shown in Fig. 1, with the addition of N, an inter-band is formed between VB and CB of ZnO, resulting in the decrease in the bandgap energy as well as the generation of a large number of holes in VB which converts the n-type to the p-type semiconductor [12].

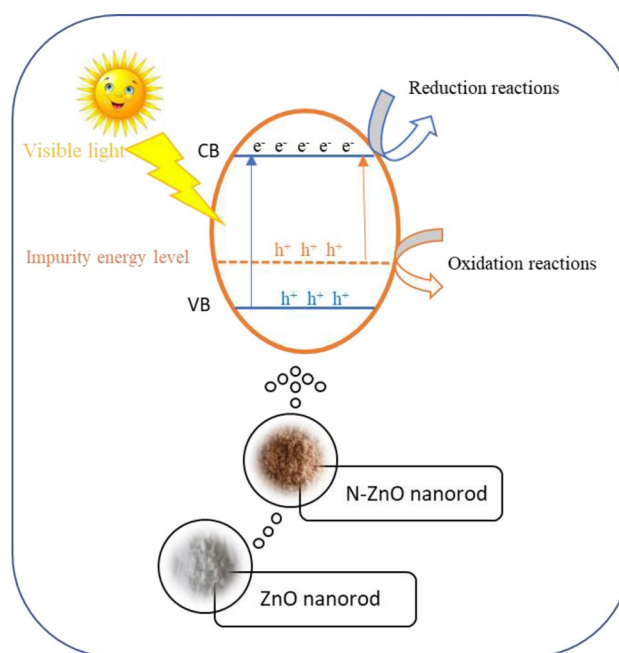


Fig. 1 Schematic energy level diagram of N-doped ZnO for a photochemical reaction

The construction of the C–S bond is a versatile transformation in synthetic and medicinal chemistry due to the biological properties of obtained sulfur compounds [13, 14]. Among the various approaches for the synthesis of organosulfur compounds, the direct thiocyanation of aromatic and heteroaromatics is most popular owing to the presence of aryl thiocyanates in the building blocks of many biologically active heterocycles and agrochemical compounds [15]. To date, many methods have been developed for electrophilic thiocyanation using thiocyanate salt in the presence of CAN, hypervalent iodine reagents, oxone, Mn(OAc), or other oxidants [16–23]. However, these methods typically suffer from some drawbacks, such as using stoichiometric oxidants or generating large amounts of heavy metal wastes [16–23]. In another hand, phenols can act as scavengers to trap the photogenerated holes in the valence band of semiconductors, so the thiocyanation of phenols using semiconductors is a challenging process requiring a suitable catalyst. In this study, we demonstrated the effect of N-doping in photocatalyst properties of ZnO nanorod in thiocyanation of indoles and phenols under visible-light irradiation.

2 Results and discussion

First, several N-doped ZnO with different content of nitrogen using urea as nitrogen source were synthesized based on our previous work [24]. To evaluate the nitrogen content, each of the synthesized catalysts was analyzed by CHNS

analysis. Accordingly from the data obtained by CHNS analysis the weight ratios (in grams) of ZnO and urea with 0.5:1, 0.5:2, 0.5:4, and 0.5:8 ratio have 0.3%, 0.32%, 0.38%, and 0.45% nitrogen, respectively. The obtained pink-colored materials are shown in Fig. 2. Based on the UV–Vis diffuse reflectance analysis it was found that the ZnO nanorod (NRs) with a higher content of nitrogen (0.45% N-doped) could significantly improve the structure of ZnO by shifting the absorption intensity peak in the visible region (Fig. 2). Therefore, this material was chosen as an appropriate photocatalyst for our studies.

The band gaps were determined by comparing the UV–Vis DRS spectra of prepared materials. Figure 3a shows the UV–Vis DRS of the pure and 0.45% N–ZnO NRs. While the pure ZnO showed absorption cut off the edge at 385 nm related to the bandgap of 3.25 eV, the nitrogen-doped ZnO showed the absorption in the visible region (491 nm), owing to the impurity of N 2p states [25]. The bandgap between Zn 3d and impurity N 2p is 2.52 eV calculated by equation $E_g = 1240/\lambda_{max}$, E_g the bandgap and λ the wavelength. Based on these observations we can discuss two bandgaps after nitrogen doping as shown in Fig. 3b: (1) bandgap between

Zn 3d and a mixture of N 2p and O 2p states and (2) band-gap between Zn 3d and O 2p. However, only the bandgap between Zn 3d and the mixture of N 2p and O 2p states can be excited by visible light.

2.1 XRD

The diffractogram of the pure ZnO and 0.45% N–ZnO NRs is shown in Fig. 4. It is observed that ZnO has a wurtzite phase (JCPDF: 891,397) in both samples. No significant peak for nitrogen is observed in N–ZnO NRs which suggests the possibility of introduction of nitrogen into the ZnO lattice without affecting the ZnO crystal structure. However, the XRD peaks of 0.45% N–ZnO NRs are found to be shifted to the higher θ values [26]. N doping shifts the diffraction peak towards a higher angle which was attributed to the larger bond length of Zn–O than that of Zn–N [27–29]. The particle size of 0.45% N–ZnO NRs as evaluated by the Scherrer formula is about 48.63 nm, while that of the pure ZnO is about 49.5 nm. The reduction of particle size may be attributed to the incorporation of nitrogen in ZnO.

2.2 FT-IR spectrum

Figure 5 shows the FT-IR spectrums of undoped ZnO and 0.45% N–ZnO NRs in the region of 400–4000 cm^{-1} [30]. There is broadband at 3410 cm^{-1} that indicates the presence of –OH groups of absorbed water during the preparation process. The band arising from the bonding between Zn–O (473 cm^{-1} , 532 cm^{-1}) is clearly represented. FT-IR spectrum shows the presence of stretching vibrational bond C–O (1650 cm^{-1}), C–H (1381 cm^{-1}). In the FT-IR spectrum also there is no peak corresponding to nitrogen which accords well with the XRD analysis. This may be due to the low nitrogen doping in ZnO. The intensity of stretching vibrational bond of O–H (3422 cm^{-1}), and stretching vibrational bond C–O (1650 cm^{-1}), C–H (1381 cm^{-1}) peaks in 0.45%

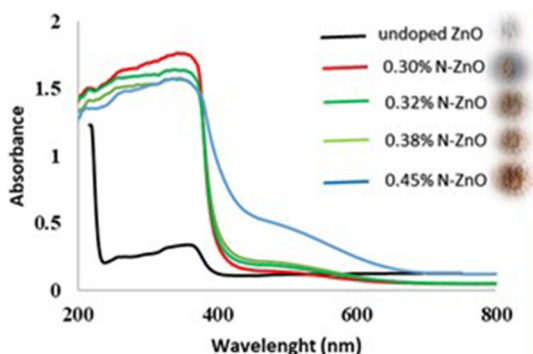
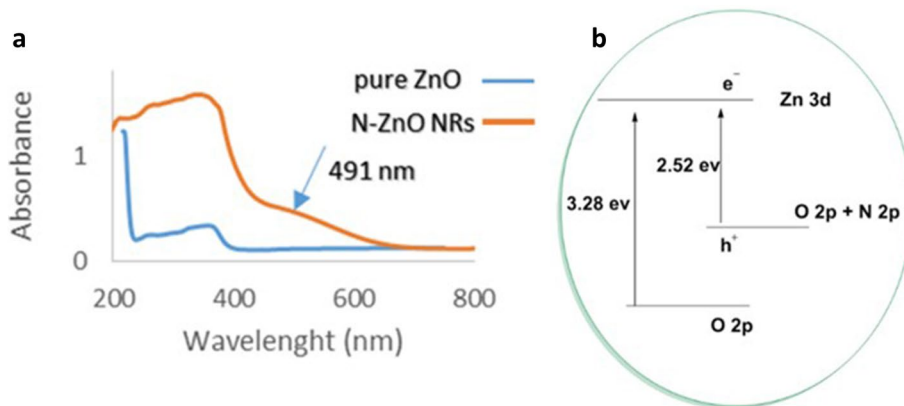


Fig. 2 UV–Vis diffuse reflection absorption spectra of five type synthesized samples

Fig. 3 a UV–Vis diffuse reflectance spectra of the pure and 0.45% N–ZnO NRs. b Proposed band structure of nitrogen-doped ZnO, valence band O 2p, and a mixture of O 2p and N 2p



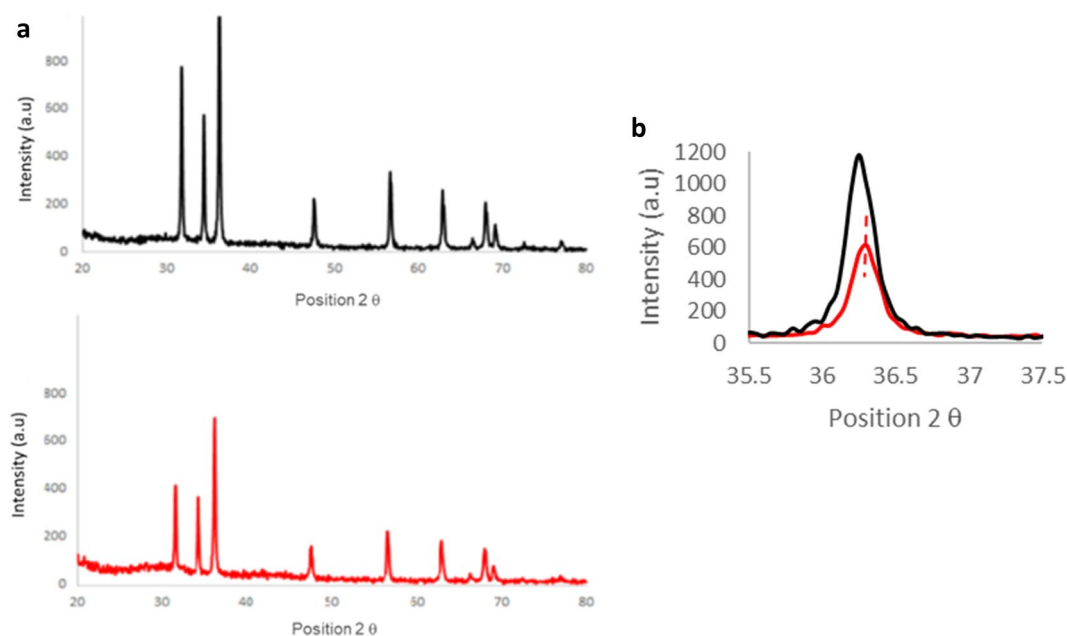


Fig. 4 **a** XRD pattern of the pure ZnO and 0.45% N-ZnO NRs. **b** Shifts in peak position is depicted through the enlarged view of (101) peaks for pure and 0.45% N-ZnO NRs

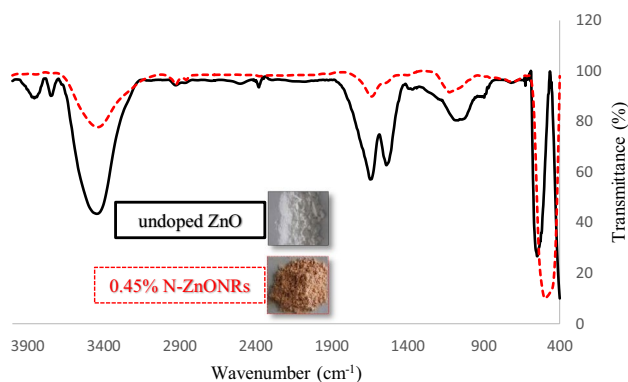


Fig. 5 FT-IR spectrum of undoped ZnO and 0.45% N-ZnO NRs

N-ZnO NRs lower compared to undoped ZnO. This may be due to exposure to furnace heat.

2.3 SEM and TEM

We have also used the SEM to directly analyze the morphology of the 0.45% N-ZnO NRs nanostructure. The SEM image of freshly synthesized 0.45% N-ZnO NRs is shown in Fig. 6a. The nano-rod surface morphology could be clearly seen with a wide range of sizes. To further study microscopic morphology and structure information, the TEM analysis of 0.45% N-ZnO NRs has been also performed, as shown in Fig. 6b.

Fig. 6 **a** SEM. **b** TEM images 0.45% N-ZnO NRs

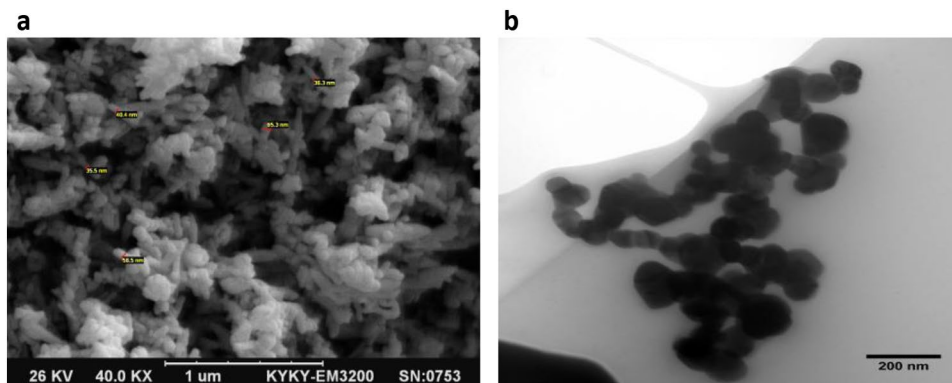


Table 1 Results of BET surface area measurements for 0.45% N-ZnO NRs

BJH adsorption summary	
Surface area	9.554 m ² /g
Pore volume	0.072 cc/g
Pore Diameter Dv(d)	1.29 nm
BET summary Surface Area	7.823 m ² /g

2.4 BET

The specific surface area of 0.45% N-ZnO NRs was measured by BET analysis that is shown in Table 1. The BET surface area of 0.45% N-ZnO NRs powder was found to be 7.823 m²/g, whereas the BJH adsorption surface area of pores was 9.554 m²/g. The single point total pore volume was found to be 0.072 cc/g.

In continuation of our interest in C–S bond formation, particularly thiocyanation reaction, we first examined the optimal 0.45% N-ZnO NRs in thiocyanation of indoles. To this end, the reaction of 1*H*-indole and ammonium thiocyanate was selected as a model reaction for further investigations (Table 2). It was observed that solvent had a great effect on the yield of the reaction. While no desired product was obtained in common solvents such as EtOH, H₂O, and DMSO, in ethyl acetate the yield was improved under irradiation with 15 W CFL (Table 2, entry 8). Then the reaction was carried out using different amounts of 0.45% N-ZnO NRs, 3 mg of the photocatalyst was the best choice, delivering the desired product in 84% yield within 24 h (Table 2, entry 10). The yield of the reaction reduced with ZnO nanorod and 38% N-ZnO as photocatalyst (Table 2, entries 9 and 10), indicating the key role of N-doping in photocatalytic properties of ZnO. To evaluate the performance of the photocatalyst, the model reaction was tested in the absence of photocatalyst and only 10% yield was obtained (Table 2, entry 13). While the reaction could not proceed in the absence of light, blue light showed high performance for the reaction, affording the target product in 94% yield within 16 h (Table 2, entry 18). Of note, the reaction yield significantly decreased using argon instead of oxygen atmosphere (Table 2, entry 19).

As stability and reusability are the main components of a considerable heterogeneous catalyst, we examined the recyclability and reusability of this nano photocatalyst. Using the optimization reaction condition, we evaluated the catalyst activity in the thiocyanation reaction of indole with ammonium thiocyanate. For this purpose, after each run, the catalyst was separated by centrifugation, washed with water and ethanol, dried, and used for the next run. The photocatalyst was applied for four runs without any decrease in photocatalytic activities to the preparation of the desired

Table 2 Model reaction using 1*H*-indole and ammonium thiocyanate^a

Entry	Cat (x mg)	solvent	Light	Yield % ^b
1	0.45% N-ZnO (0.010 g)	CH ₃ CN	CFL (15 W)	13
2	0.45% N-ZnO (0.010 g)	CH ₃ Cl	CFL (15 W)	39
3	0.45% N-ZnO (0.010 g)	THF	CFL (15 W)	44
4	0.45% N-ZnO (0.010 g)	DMSO	CFL (15 W)	15
5	0.45% N-ZnO (0.010 g)	DMF	CFL (15 W)	20
6	0.45% N-ZnO (0.010 g)	EtOH	CFL (15 W)	18
7	0.45% N-ZnO (0.010 g)	H ₂ O	CFL (15 W)	12
8	0.45% N-ZnO (0.010 g)	EtOAc	CFL (15 W)	59
9	0.45% N-ZnO (0.005 g)	EtOAc	CFL (15 W)	68
10	0.45% N-ZnO (0.003 g)	EtOAc	CFL (15 W)	84
11	0.38% N-ZnO (0.003 g)	EtOAc	CFL (15 W)	76
12	Undoped ZnO(0.003 g)	EtOAc	CFL (15 W)	27
13	–	EtOAc	CFL (15 W)	10
14	0.45% N-ZnO (0.003 g)	EtOAc	Blue LED 12 W	94
15	0.45% N-ZnO (0.003 g)	EtOAc	Green LED 12 W	38
16	0.45% N-ZnO (0.003 g)	EtOAc	Red LED 12 W	0
17	0.45% N-ZnO (0.003 g)	EtOAc	–	0
18 ^c	0.45% N-ZnO (0.003 g)	EtOAc	Blue LED 12 W	94
19 ^d	0.45% N-ZnO (0.003 g)	EtOAc	Blue LED 12 W	10

^aReaction conditions: 1*H*-indole (0.10 mmol), ammonium thiocyanate (0.30 mmol), 0.45% N-ZnO NRs (0.003g) in EtOAc (1 mL)

^bIsolated yields

^cDuring 16 h

^dUnder Ar atmosphere

product; moreover, the XRD pattern and FT-IR spectrum of the recovered catalyst after the last run was compared to the fresh catalyst and no considerable change in the structure of the photocatalyst was observed (Fig. 7).

With optimum conditions in hand, we screened the substrate scope of the reaction (Table 3). In most cases, the desired products obtained in high yields, only in the case of 2-methyl indole **1c** due to steric hindrance lower yield was observed (Tables 3, 1c).

Then we extend our work toward the thiocyanation of phenols. In this case similar to indole the best reaction conditions were obtained in EtOAc using 45% 0.45% N-ZnO NRs at room temperature, but in longer reaction time (48 h) (Table 4). As shown in Table 3, thiocyanation predominantly took place at the *para* position of phenols. It was observed that the reaction was sensitive to the nature of substituents, and phenols bearing electron-donating groups such as methyl and methoxy gave higher yields (Table 4, 4d–g).

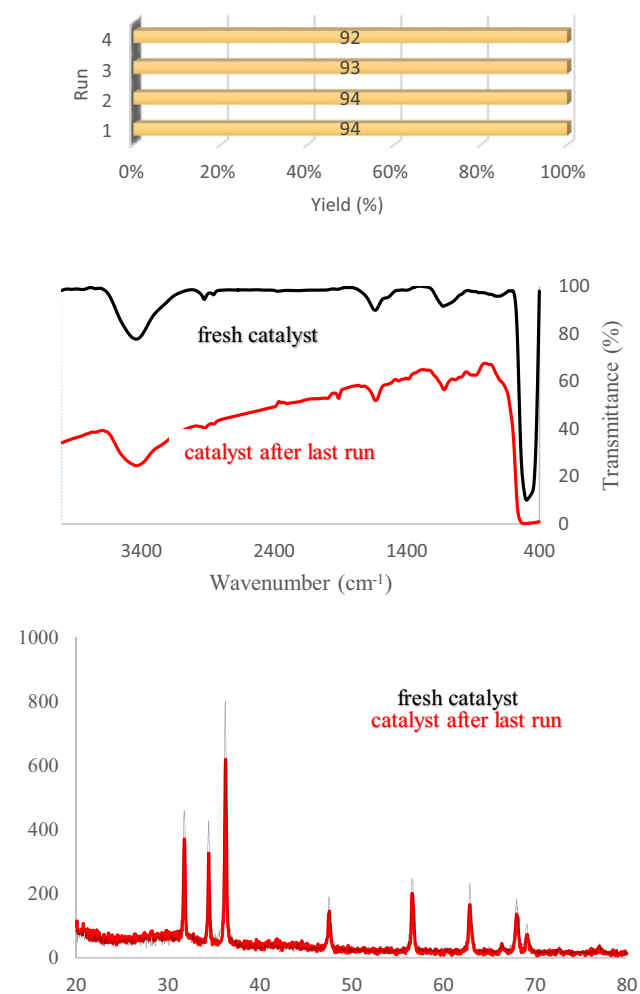
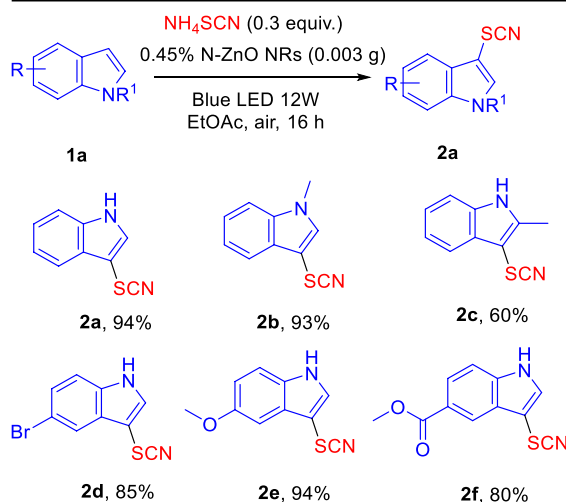


Table 3 Thiocyanation reaction of indole derivatives



Reaction conditions: 1H-Indole (0.5 mmol), ammonium thiocyanate (1.5 mmol), 0.45% N-ZnO NRs (15 mg), EtOAc (5 mL)

Isolated yields

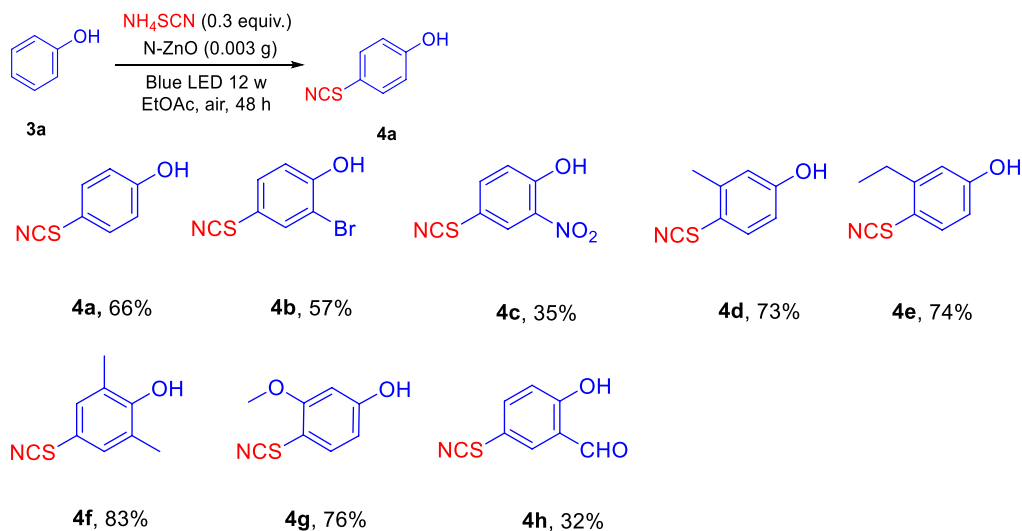
To gain insight into the mechanism of the reaction several control experiments were conducted under the optimized conditions (Scheme 1). When the radical-trapping agent TEMPO (2 equiv) was added to reaction mixtures under the relevant standard conditions, no product was observed. In addition, triethanolamine (TEA) as a scavenger to trap the holes were examined, and no reactivity was observed for the 0.45% N-ZnO NRs (Scheme 1). These results suggested that this process was likely progressed through the radical process.

Based on these results we proposed a mechanism as shown in Scheme 2. First, under visible light irradiation, electron and hole pairs were generated between N 2p states and the conduction band of Zn 3d. The excited electrons in the conduction band moved to the surface and further transfer to surface-adsorb oxygen, producing superoxide anion. Subsequently, a SET process between $\cdot\text{SCN}^-$ and hole affords $\cdot\text{SCN}$. Electrophilic addition of this radical to **1a** resulted in intermediate **A** which oxidized to give cation intermediate **B**. Finally, rearomatization of **B** followed by deprotonation delivered the target product **2a**.

It should be noted that the 0.45% N-ZnO NRs photocatalyst could be separated and recovered conveniently by centrifugation from the reaction mixture, and used in the next run. Following this procedure, the catalyst was recycled and reused effectively four times (for two model reactions, indole, and phenol) without any decrease in photocatalytic activities.

For comparison, we provide a table (Table 5) of available visible light catalysts reports for thiocyanation of indoles and phenols and comparing our and the previous results. As

Fig. 7 a Recyclability, b FT-IR spectrum, and c XRD pattern of the recovered 0.45% N-ZnO NRs after four-cycle

Table 4 Thiocyanation of phenol under visible light over 0.45% N-ZnO NRs NRs.

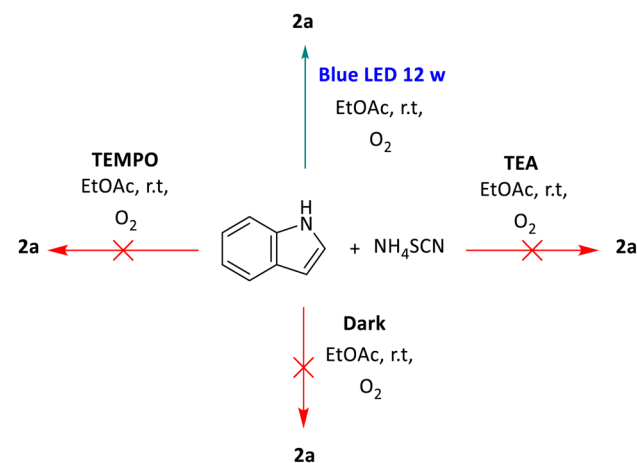
^aReaction conditions: Phenol (0.1 mmol), ammonium thiocyanate (0.3 mmol), 0.45% N-ZnO NRs (0.003 g), solvent (1 mL)

^bIsolated yields

can be seen in our work we use a heterogeneous catalyst and also a greener solvent that are the highlight and significance of the present work.

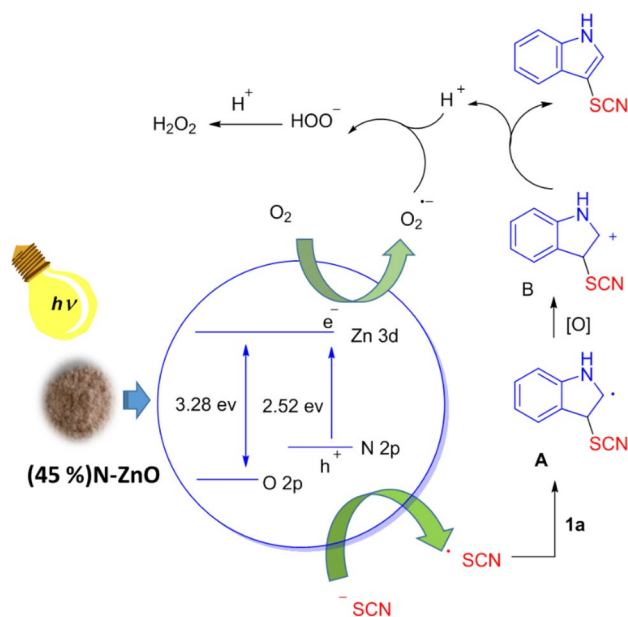
3 Conclusion

In summary, in this study we explored the effect of N-doping in photochemical properties of ZnO nanorods, we have also developed regioselective thiocyanation of various indoles and phenols using reusable photocatalyst 0.45% N-ZnO NRs



Scheme 1 Control experiments

nanorod in extremely mild reaction conditions together with moderate to good yields. Mechanistic studies confirmed that this reaction progressed through a photoredox radical pathway.



Scheme 2 Proposed mechanism

Table 5 Thiocyanation of indoles and phenols under visible light irradiation over photocatalysts using air as oxidant at r.t

Catalyst (substrate for thiocyanation)	Time (h)	Solvent	Irradiation	Yield	Refs
TiO ₂ /MoS ₂ (indole)	16	CH ₃ CN	Visible light 14w CFL	93%	[31]
Rose Bengal (indole)	18–48	THF	Visible light 14 W CFL	Up to 98%	[32]
ARS-TiO ₂ (indole)	20	THF	Blue LEDs 12w	93%	[33]
ARS-TiO ₂ (phenol)	24	THF	Blue LEDs 12w	92%	[33]
0.45% N–ZnO NRs (indole)	16	EtOAc	Blue LEDs 12w	94%	This work
0.45% N–ZnO NRs (phenol)	48	EtOAc	Blue LEDs 12w	83%	This work

Supplementary Information The online version contains supplementary material available at <https://doi.org/10.1007/s43630-021-00068-0>.

Acknowledgements This work was supported by the Shiraz University.

Author contributions The manuscript was written through the contributions of all authors. All authors have approved the final version of the manuscript.

Declarations

Conflict of interest There are no conflicts of interest to declare.

References

- Rajeshwara, K., Osugi, M. E., Chanmanee, W., Chenthamarashan, C. R., Zanoni, M. V. B., Kajitvichyanukul, P., & Krishnan-Ayer, R. (2008). *Journal of photochemistry and photobiology C: photochemistry reviews*, 9, 171–192.
- Rehman, S., Ullah, R., Butt, A. M., & Gohar, N. D. (2009). *Journal of Hazardous Materials*, 170, 560–269.
- Chungui, T., Qi, Z., Aiping, W., Meijia, J., Zhenglan, L., Baojiang, J., & Honggang, F. (2012). *Chemical Communications*, 48, 2858–2860.
- Wang, G., Chen, D., Zhang, H., Zhang, J. Z., & Li, J. H. (2008). *Journal of Physical Chemistry*, 112, 8850–8855.
- Hornyak, G. L., Dutta, J., Tibbals, H. F., & Rao, A. (2008). *Introduction to nanoscience*. Boca Raton: CRC Press.
- Lin, H., Huang, C. P., Li, W., Ni, C., Shah, S. I., & Tseng, Y. H. (2006). *Applied Catalysis B: Environmental*, 68(1–2), 1–11.
- Xu, Z., Chenghua, S., Hua, Y., Zhi, G. C., Zheng, X., Delai, Y., Gao, Q. L., Xinyong, L., & Lianzhou, W. (2013). *Journal of Physical Chemistry C*, 117, 4937–4942.
- Chen, S., Zhao, W., Zhang, S., & Liu, W. (2009). *Chemical Engineering Journal*, 148, 263.
- Hongchun, Q., Weiyang, L., Yujing, X., Tao, H., & Appl, A. C. S. (2011). *Mater. Interfaces*, 3, 3152–3156.
- Swapna, R., & Santhosh Kumar, M. C. (2013). *Materials Science and Engineering B*, 178(16), 1032–1103.
- Chen, X., Lou, Y. B., Samia, A. C. S., et al. (2005). *Advanced Functional Materials*, 15(1), 41–49.
- Silva, I. M. P., Byzynski, G., Ribeiro, C., et al. (2016). *Journal of Molecular Catalysis A: Chemical*, 417, 89–100.
- Mishra, C. B., Kumari, S., & Tiwari, M. (2015). *European Journal of Medicinal Chemistry*, 92, 1–34.
- Ayati, A., Emami, S., Asadipour, A., Shafiee, A., & Foroumadi, A. (2015). *European Journal of Medicinal Chemistry*, 97, 699–718.
- Piscitelli, S. C., Goss, T. F., Wilton, J. H., D'andrea, D. T., Goldstein, H., & Schentag, J. J. (1991). *Antimicrobial agents and chemotherapy*, 35(9), 1765–1771.
- Rezayati, S., & Ramazani, A. (2020). *Tetrahedron*, 76(36), 131382.
- Majedi, S., Sreerama, L., & Vessally, E. (2020). and F. *Behmgham J. Chem. Lett.*, 1(1), 25–31.
- Nair, V., & Nair, L. G. (1998). *Tetrahedron Letters*, 39, 4585–4586.
- Nair, V., George, T. G., Nair, L. G., & Panicker, S. B. (1999). *Tetrahedron Letters*, 40, 1195–1196.
- De Mico, A., Margarita, R., Mariani, A., & Piancatelli, G. (1996). *Tetrahedron Letters*, 37, 1889–1892.
- Yadav, J. S., Reddy, B. V. S., & Krishna, B. B. M. (2008). *Synthesis*, 2008(23), 3779–3782.
- Wu, G., Liu, Q., Shen, Y., Wu, W., & Wu, L. (2005). *Tetrahedron Letters*, 46, 5831–5834.
- Pan, X.-Q., Lei, M.-Y., Zou, J.-P., & Zhang, W. (2009). *Tetrahedron Letters*, 50, 347–349.
- Koohgard, M., Sarvestani, A. M., & Hosseini-Sarvari, M. (2020). *New Journal of Chemistry*, 44, 14505–14512.
- Irie, H., Washizuka, S., Yoshino, N., & Hashimoto, K. (2003). *Chemical Communications*, (11), 1298–1299.
- Minami, T., Sato, H., Nanto, H., & Takata, S. (1986). *Japanese Journal of Applied Physics*, 25, L776.
- Zhu, X., Wu, H. Z., Qiu, D. J., et al. (2010). *Optics Communications*, 283(13), 2695–2699.
- Meng, A., Li, X., Wang, X., et al. (2014). *Ceramics International*, 40(7), 9303–9309.
- Söllradl, S., Greiwe, M., Bukas, V. J., et al. (2015). *Chemistry of Materials*, 27(12), 4188–4195.
- Rajbongshi, B. M., Ramchiary, A., & Samdarshi, S. (2014). *Materials Letters*, 134, 111–114.
- Wang, L., Wang, C., Liu, W., Chen, Q., & He, M. (2016). *Tetrahedron Letters*, 57(16), 1771–1774.
- Fan, W., Yang, Q., Xu, F., & Li, P. (2014). *Journal of Organic Chemistry*, 79(21), 10588–10592.
- Koohgard, M., Hosseinpour, Z., Sarvestani, A. M., & Hosseini-Sarvari, M. (2020). *Catalysis Science and Technology*, 10(5), 1401–1407.

Authors and Affiliations

Mona Hosseini-Sarvari¹  · Abdollah Masoudi Sarvestani¹

¹ Nano Photocatalysis Lab, Department of Chemistry, Shiraz University, Shiraz 7194684795, Islamic Republic of Iran